

Jie Wu · Yuxing Ben · Hsueh-Chia Chang

## Particle detection by electrical impedance spectroscopy with asymmetric-polarization AC electroosmotic trapping

Received: 20 July 2004 / Accepted: 22 September 2004 / Published online: 6 April 2005  
© Springer-Verlag 2005

**Abstract** Recently, considerable interest and effort have been devoted to the on-site detection of low-concentration pathogenic bacteria in order to deter infectious diseases and bioterrorism. Conventionally, bacteria detection involves culturing, which is time-consuming and unfeasible under field conditions. Microfluidic devices with integrated electrical detection will enable fast, low-cost, and portable sensing and processing of biological and chemical samples. AC electroosmosis (EO) is well-suited for integration into microsystems due to its low-voltage operation and no-moving-part implementation and microelectrical impedance spectroscopy can be integrated with AC EO for particle manipulation, leading to enhanced sensitivity due to a reduction of the transport time to the detector. Experiments are performed to find optimal conditions for obtaining particle and bacterial assembly lines on electrodes by AC EO and preliminary results show good resolution at a concentration of  $10^4$  bacteria/ml, indicating that combining AC EO with impedance measurement can improve the sensitivity of particle electrical detection.

**Keywords** AC electroosmosis · Bacteria detection · Biosensing electrokinetics · Microimpedance sensor

### 1 Introduction

On-site rapid bacteria detection and identification have become a matter of growing concern globally. Diseases from pathogenic bacteria are the major cause of death in many developing countries, accounting for nearly 40% of the total 50 million annual estimated deaths worldwide. In fact, the incidences of human diseases caused by food-borne bacterial pathogens, such as *Salmonella typhimurium*, *Escherichia coli*, *Staphylococcus aureus*, and *Campylobacter jejuni*, have not decreased since 1994 (Ivnitski et al. 2000), which can be attributed to rising antibiotic resistance, strain variations, and the increased movement of people and products across the globe. The Centers for Disease Control and Prevention (CDC) estimates 76 million food-borne illnesses each year in the US, with 325,000 hospitalizations and 5,000 deaths (Mead et al. 2000). Contaminated drinking water, beaches, and improperly disinfected swimming pools (Keene et al. 1994) have also been implicated as sources of infection. The United States Department of Agriculture (USDA) estimates the cost of human illness in the USA for the top six bacterial pathogens at US\$9–13 billion annually due to medical costs and lost productivity (Buzby et al. 1996). Pathogenic bacteria are also a rising concern from the perspective of national security, as a number of them fall into the category of biological warfare agents, such as *Bacillus anthracis* (causing Anthrax) (Compton 1987). From September to November 2001, a total of 23 confirmed/suspected cases of bioterrorism-related anthrax (10 inhalation, 13 cutaneous) occurred in the United States. A study by the CDC shows that an intentional release of anthrax by bioterrorists in a major US city would result in an economic loss of US\$477.8 million to US\$26.2 billion per 100,000 persons exposed (Shah and Wilkins 2003).

However, one difficulty in detecting pathogenic bacteria is that they are generally present at very dilute concentrations ( $< 100$  colony-forming units (CFU) per ml, which assumes each bacterium develops into one

J. Wu · Y. Ben · H.-C. Chang (✉)  
Center for Micro-fluidics and Medical Diagnostics,  
Department of Chemical and Biomolecular Engineering,  
University of Notre Dame, Notre Dame, IN 46556, USA  
E-mail: chang.2@nd.edu  
Tel.: +1-574-6315697  
Fax: +1-574-6318366

J. Wu  
Department of Electrical & Computer Engineering,  
The University of Tennessee,  
Knoxville, TN 37996, USA

colony during culturing). An infectious dose may be just one microorganism among many other benign bacteria. For example, the level of *E. coli* O157:H7 that is considered “acceptable” by the USDA for poultry products is fewer than 100 CFU/ml of whole carcass rinse (400 ml). An *E. coli* level of 100–1,000 CFU/ml is considered marginal, and levels higher than 1,000 CFU/ml are considered unacceptable (Russell 2003).

Currently, real-time bacteria detection has a typical sensitivity in the range of  $10^6$ – $10^7$  CFU/ml (Ivnitski et al. 1999). One reason is that biosensors function effectively as detectors only when the bacteria or viruses are proximal and only when sufficient particles are present to stimulate signal generation. For such diluted samples, the conventional gold standard is the plate-counting; that is, selectively culturing the pathogen of choice to detectable levels while limiting the growth of competing microflora. This procedure is time-consuming (24–48 h of enrichment prior to analysis) (Kourkine et al. 2003) and often unfeasible for field testing.

Realizing that the barrier to detection sensitivity could possibly be overcome by reducing the diffusion time from the bioparticles to the sensors, so instead of elaborating on sensing mechanisms, this work seeks to improve the sensitivity in real-time bacteria detection with a system approach, by incorporating electroosmotic fluid manipulation and collection with sensing mechanisms.

Electrical impedance spectroscopy (EIS) is adopted as the detection method in our concept. EIS systems are simple to construct, compatible with microfabrication, as well as being reliable with no moving parts (Gale and Frazier 1999). There have been reports on microfabricated EIS prototypes intended for microfluidic systems, which are based on changes in solution conductivity (Ayliffe et al. 1999; Ayliffe and Rabbitt 2003; Gomez et al. 2001).

Here, we report on an EIS scheme that utilizes AC electroosmosis (EO) to concentrate particles for enhanced selectivity. When an AC electric field is applied to electrodes submerged in electrolytes, particles suspended in fluid could experience forces, such as dielectrophoretic force or electroosmotic force. Due to small dimensions of microfabricated electrodes, sufficient electric field strength for dielectrophoresis (DEP) or EO can be obtained with relatively low voltages applied over the electrodes. Our goal is to use AC electroosmotic forces to bring particles from the bulk of the suspension to the electrode surface, where the presence of particles has a larger impact on impedance measurements than in the bulk.

It has been well documented that DEP can be used for the manipulation and characterization of particles, and the separation of mixtures, such as cells, bacteria, and latex spheres (Auerswald and Knapp 2003; Hughes and Morgan 1999; Morgan et al. 1999; Ramos et al. 1999). However, DEP is size-sensitive and of rather short range; therefore, it is not effective for manipulating micron and submicron bioparticles like bacteria and

viruses more than 20  $\mu\text{m}$  away from the electrodes. On the other hand, electroosmotic motion has no dependence on particle size and scales much more favorably with the distance from the electrode ( $1/r$  vs.  $1/r^3$  for DEP). Therefore, EO force is particularly advantageous for collecting micron/submicron particles from the electrolyte. We use AC EO to direct particles to certain locations, and in doing so, greatly enrich the local particle concentration at the electrode surface to a detectable level. With our preliminary results, this technique holds strong promise in realizing a practical on-site bioparticle detection system. There are prior observations of particle aggregation on the electrode surface (Trau et al. 1996; Yeh et al. 1997) and the concentration of bacteria on electrodes (Hoettges et al. 2003; Wong et al. 2003) by EO flows, where the particle deposition was attributed to DEP and surface forces. We have investigated the electric field distribution around electrodes and are able to offer a new perspective on particle concentration that will be given later in the paper.

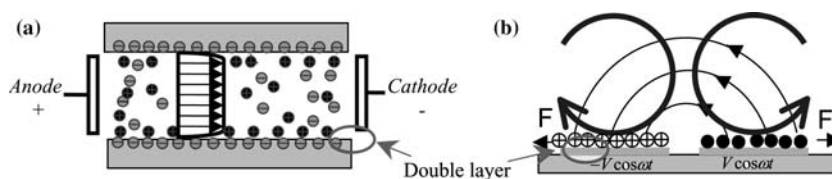
Since AC scanning signals are adopted in EIS detection, AC electrokinetics can be readily combined with EIS. Measuring cell impedance at an AC potential appropriate for inducing surface flow and particle assembly, we have observed an increased differentiation of impedances between bacteria suspensions and buffer solutions. Within 1 minute, we are able to induce a bacterial self-assembly line on each electrode. The bacterial lines represent an increase in concentration by four orders of magnitude relative to the bulk. In addition, impedance spectroscopy using the same electrodes that drive the EO flow indicates that the bacteria lines significantly alter the surface conductance and capacitance of the electrodes. Using just one pair of pumping/sensor electrodes, the sensitivity of our detector can reach  $10^4$  bacteria per ml.

---

## 2 Particle assembly by AC electroosmosis

EO is the fluid motion induced by the movement of surface charges at the solid–liquid interface under the influence of electric fields. Most materials will acquire fixed surface charges when coming into contact with a fluid that contains ions (either an electrolyte or a dielectric liquid with ionic impurities or generated locally via reactions). By electrostatic attraction, the surface charges attract counter-ions from the solution and repel co-ions from the surface to maintain local charge neutrality. Consequently, excess charge is built up near the solid surface, thus, forming an electrical double layer or a capacitor, as in electronics. The ions in the liquid phase of the double layer are mobile, and will migrate under the influence of an electric field tangential to the electrode surface. Due to viscosity, fluid surrounding the ions will also move, resulting in so-called electroosmosis. This phenomenon has been applied to build DC EO pumps (Chen and Santiago 2002), where the electric field

**Fig. 1** Schematics of **a** DC electroosmosis and **b** AC electroosmosis by capacitive charging



tangential to the double layer is imposed by two electrodes at the ends of microchannels, as shown in Fig. 1a. To achieve sufficient electric field strengths over the length of the microchannels, DC EO pumps have to use high voltages on the order of kilovolts, which causes serious water electrolysis, bubble generation, and pH gradients (Minerick et al. 2002) at the electrodes.

Another type of EO is AC EO (Ramos et al. 1998), which is a relatively new research area in microfluidics. Because electrode arrays are energized with time-varying potentials, undesirable reactions at the electrodes are suppressed due to interruption and relaxation of the reactions. Similar to DC EO, AC EO is also generated by exerting a force on double-layer charges at the solid-liquid surface by tangential electric fields. In AC EO, the charges in the electrical double layer are induced by the electric potentials over electrodes instead of surface charges in DC EO, and the applied potentials also provide tangential electric fields to drive the ions. Because the electric fields of a symmetric electrode pair exhibit mirror symmetry, and charges in the double layer and electric fields change signs simultaneously, AC EO produces steady counter-rotating local vortices above the electrodes (Green et al. 2002), as shown in Fig. 1b. The bold arrows indicate the flow directions induced by capacitive charging. For microfluidic applications, AC EO has some advantages over DC EO, in that it uses low-magnitude voltages (a few volts), and its active elements, the electrodes, are compatible with microfab-

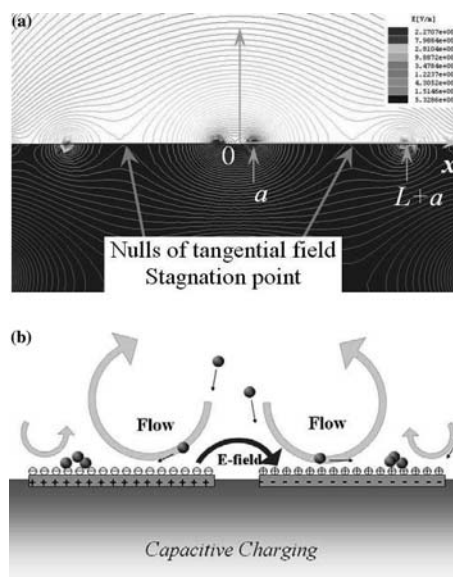
rication and can be readily integrated with control circuits and microfluidic elements, for example, microchannels and microchambers.

Our work suggests that particles prefer to deposit at certain locations due to local gradients of electric fields at the electrode surface, as shown in Fig. 2. The stagnation lines are located at positions where there is a change in the tangential field direction, which is  $1/\sqrt{2}$  of the electrode width away from its inner edge for isolated, wide electrodes, as shown in Fig. 2a. Because flow directions depend on the tangential fields, four counter-rotating vortices were formed at the electrode surface, and the stagnation takes place at locations where tangential fields become zero, as shown in Fig. 2b. This technique has been extrapolated to attract bioparticles from the bulk of a suspension to electrode surface, thus, reducing the diffusion time of bioparticles to the detectors. It will be shown in this paper the difference in detected signals with and without AC EO particle collection.

### 3 Asymmetric polarization AC electroosmosis

In the AC EO discussed above, the charges at the electrode surfaces are counter-ions to the electrode potentials, attracted from the electrolyte to screen the electrode potential. This electrode polarization is known as capacitive charging or induced charging (Squires and

**Fig. 2** **a** Electric field distribution above a pair of planar electrodes. The tangential  $E$  fields change sign at  $1/\sqrt{2}$  of the electrode width (stagnation point). (Axes show relative dimensions.) **b** With capacitive charging, four counter-rotating vortices are formed above the electrodes due to changes in tangential electric fields. At an appropriate strength of electrode polarization, particles aggregate at the stagnation points



Electric field distribution above a pair of planar electrodes. The tangential component changes sign at  $1/\sqrt{2}$  of electrode-width (stagnation point). (Axes: relative dimensions)

With capacitive charging, four counter-rotating vortices are formed above the electrodes due to changes in tangential electric fields. At an appropriate strength of electrode polarization, particles aggregate at the stagnation points.

Bazant 2004), and is the only mechanism reported in the literature. However, our work at the Center for Microfluidics and Medical Diagnostics (CMMD) at Notre Dame indicates that there exist other AC electrode processes, which are represented by surface flows in opposite directions to those produced by capacitive charging. The hypothesis for this phenomenon is that, at an appropriate electrode potential, co-ions instead of counter-ions are generated from electrochemical reactions at the electrodes following Faraday's law; therefore, it is dubbed as Faradaic charging here.

Capacitive and Faradaic charging differ in the following aspects, which are the basis of the proposed concept of asymmetric-polarization (A-P) AC EO. (1) With electrodes positively biased, the two charging mechanisms produce ions of opposite signs in an electrical field, which, in turn, result in EO flows in opposite directions. (2) Capacitive charging cannot produce a charge density exceeding the equilibrium charge density on the electrode side, while Faradaic charging can produce charge densities of several orders of magnitude beyond equilibrium values. (3) The charge densities produced by two polarizations have different dependence on the applied voltage,  $\sigma \sim V^2$  for capacitive charging and  $\sigma \sim \exp(V)$  for Faradaic charging, respectively. Since EO slip velocity is proportional to charge density in the doubly layer, EO velocity by the two polarizations exhibits similar voltage dependence. (4) Because there is a threshold voltage for Faradaic reaction to occur, capacitive charging dominates at low voltages, while Faradaic charging takes over at higher voltages with its exponential dependence on potential.

Capacitive charging and Faradaic charging coexist and compete for dominance when the electrodes are energized under certain conditions. The A-P scheme is built on the fact that the two electrodes in a pair undergo the two distinct polarization processes.

A-P AC EO is implemented by energizing electrode pairs with biased AC signals so that electrodes in a pair undergo polarizations different from each other. The

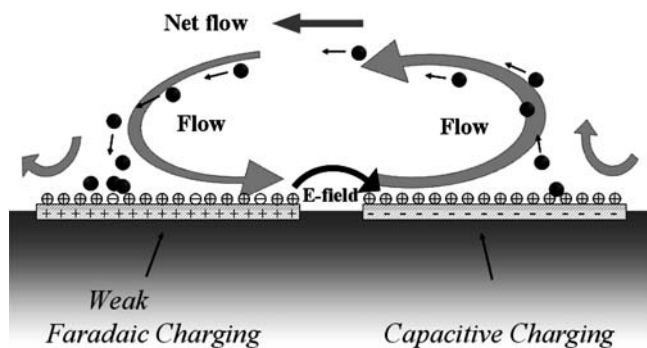


**Fig. 3** Schematic showing particle trapping by asymmetric polarization AC EO. Streamlines from capacitive charging and Faradaic charging become connected, forming a large vortex over the electrode pair. Particles are preferentially convected to the positively biased electrode

advantage of such a scheme is twofold. First, it breaks the mirror symmetry of electric fields and, consequently, that of surface flows. If Faradaic charging occurs on one electrode while capacitive charging takes place on the other, then ions of the same sign populate the electrode surface and they migrate in the same direction under the influence of the electric fields. As a result, a unidirectional flow is produced at the electrode surface.

One application of this A-P AC EO is directed particle collection; that is, particles are trapped onto a designated electrode, as schematically shown in Fig. 3. We then assume that a biased AC signal,  $V_{\text{appl}} = V_0(1 + \cos \omega t)$  is impressed over the electrodes in Fig. 3. The left electrode is always positive and more prone to Faradaic charging, while the right is always negative and subject to capacitive charging. It is presumed that, at the left electrode, the Faradaic reaction is partially compensated by the opposite capacitive polarization, leading to a weak flow. At small supercritical conditions, the streamline from the capacitive flow on the right electrode is connected to Faradaic flow on the left. A large recirculation flow exists beneath this streamline and the flow allows preferential convection of particles onto the left electrode.

Another unique feature of A-P AC EO makes it especially advantageous in trapping particles with the positively charged electrode. Because there is a DC component in the energizing signal, the scheme synthesizes DC and AC electrokinetics. Electrophoretic (electrostatic) force is exerted simultaneously with AC electrokinetic forces onto particles, colloids, and ions. Because colloidal particles and microorganisms acquire negative charges in a solution (Chang et al. 2002), particles experience electrophoretic forces, in addition to EO forces, and migrate towards positively biased electrodes. Preliminary experiments have yielded very encouraging results on particle concentration and will be discussed later.

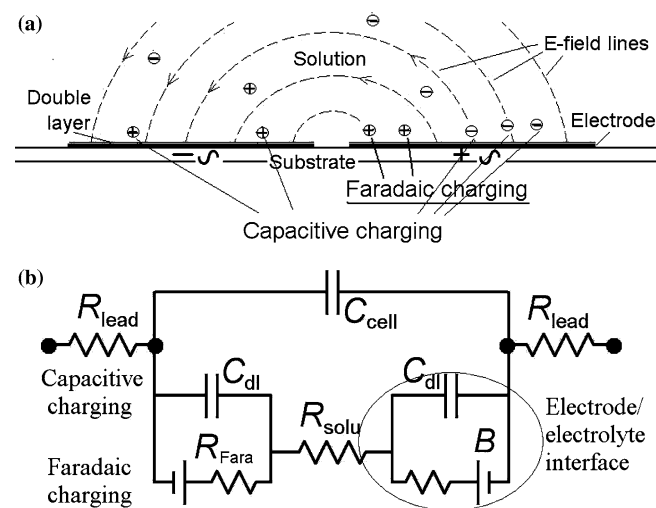


**Fig. 4** a Schematic and b electrical representation of electrode polarizations

## 4 Electrical impedance spectroscopy

For an electrochemical cell, such as those used for bio-particle detection, the impedance between the electrodes is determined by physical properties of the electrodes and the electrolyte, as well as chemical interactions between the metal and the ions in the electrolyte. Each of these current conducting processes can be represented by an electronic element. For the electrochemical cell under test (also the electrode configuration adopted in this work), as shown in Fig. 4a, an electrical equivalent circuit is developed, as shown in Fig. 4b. An appropriate equivalent circuit helps to identify the relative impacts of various impedance components at different frequencies and potentials.

In Fig. 4b,  $R_{\text{lead}}$  represents lead resistance, which arises from the thin film metal lines, bonding pads, etc.; therefore, they are in series with the electrolytic cell.  $C_{\text{cell}}$  accounts for direct capacitive coupling between the two electrodes. The value of  $C_{\text{cell}}$  depends on the dielectric properties of the electrolyte and electrode geometries. The bulk of the electrolyte obeys Ohm's law, so the bulk of the solution is modeled as a resistor  $R_{\text{solu}}$  in series with components at the interfaces of the electrodes and the electrolyte.

There are several current-conducting mechanisms at the electrode–electrolyte interface. Hydrolyzed ions at the surface of metal electrodes cause a double layer capacitance,  $C_{\text{dl}}$ , which represents a capacitive charging process. There are also electrode reactions at the interface, which is represented by a battery and a resistor in our equivalent circuit for Faradaic charging, as shown in Fig. 4b. If there is an electrode reaction, electric charges are transferred across the interface in parallel to the charging of the double layer, so the Faradic components are in parallel with  $C_{\text{dl}}$ .

The relative importance of circuit components determines the frequency response of the electrode impedance. Because of the small thickness of double layers,  $C_{\text{dl}}$  is generally much larger than  $C_{\text{cell}}$ . Therefore, at low frequencies, voltage drops mostly happen at the electrode–electrolyte interface, and the cell impedance behaves somewhat like a capacitor. However, due to electrode reactions, there is a resistive component, so the Bode plot deviates from a  $-20$  dB/decade (or  $-\text{decade}/\text{decade}$ ) downward slope. As the frequency increases, the admittance across the double layer becomes smaller and more current flows through the resistive bulk of the solution, so the impedance spectrum approaches a flat line, and that is the bulk resistance,  $R_{\text{solu}}$ . At higher frequencies, the dielectric coupling of the electrodes dominates the cell impedance, and the impedance curve becomes a  $-20$  dB/decade line again.

It can be deduced that at low to medium frequency, the interfacial impedance dominates the current conducting path and most of the applied voltage drops over the electrical double layer. So it is the frequency range

where the impedance difference from particle assembly is expected to be detected.

## 5 Experiments

The detection of particles was carried out with a pair of Ti/Au (10 nm/90 nm) parallel microelectrodes. Ti is the adhesion layer between the substrate and Au, and Au is in contact with electrolytes. Planar microfabrication techniques were used to fabricate electrodes on glass substrates. The procedure is as follows: deposit a layer of  $\text{SiN}_x$  on glass substrates to promote photoresist adhesion, apply photoresists and patterning electrodes for metal lift-off, electron-beam evaporate 0.1- $\mu\text{m}$ -thick metals, and immerse samples in acetone to obtain electrodes.

The electrodes were 20-mm long, 300- $\mu\text{m}$  wide, and 0.1- $\mu\text{m}$  thick with a 20- $\mu\text{m}$  separation.  $R_{\text{lead}}$  is calculated to be  $\sim 18 \Omega$  for Ti/Au electrodes. As the cell impedance is determined to be over several kilohms, the electric field distribution in the electrodes lengthwise is expected to be uniform. The electrode chambers were formed by sealing silicone microchambers (PC8R-0.5, Grace Bio-Labs, Inc.) over the glass slides, so an approximately 9-mm length of electrode pairs was exposed to electrolytes, and the electrode chambers have a height of 500  $\mu\text{m}$ . An HP33120 signal generator was used to apply electrical potential to electrodes.

Our previous experiments have determined the frequency and potential ranges of electrical signals for bioparticles to assemble at the stagnation positions indicated in Fig. 2b. A voltage magnitude of 1 V rms

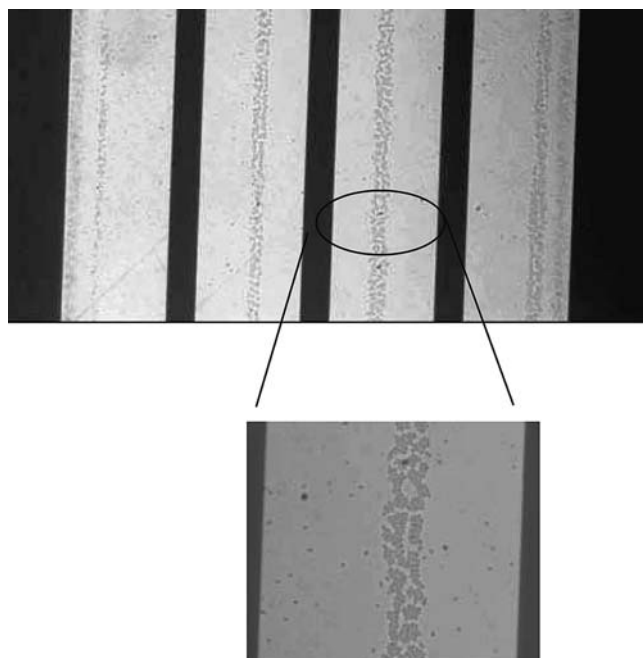


Fig. 5 Assembled *E. Coli* lines on electrodes

was determined to be optimal for observing particle motion in the DI water and tap water suspension, so the subsequent experiments were carried out at the potential level.

Bacteria *E. coli* was used to test the concept of particle collection by AC EO. Using 1 V rms at 100 Hz, lines of bacteria were formed within 30 seconds on the electrode surface from a  $4 \times 10^6$  CFU/ml tap water suspension, as shown in Fig. 5. Then, we proceeded to test the sensitivity of impedance measurements at two different potentials so as to prove that bioparticle collection by AC EO improves the detection limits.

The electrode impedances were measured with an Agilent 4294A impedance analyzer from 40 Hz to 5 MHz at an open oscillation level of 5 mV rms and 1.0 V rms. *E. coli* were resuspended in tap water of 2 mS/M at  $5 \times 10^3$  CFU/ml. The measured impedance spectra are given in Fig. 6. For the measurements at 5 mV, little difference between *E. coli* suspensions and control tap water could be detected. As a comparison, the measurements of the same samples at 1 V rms exhibit an impedance difference by a factor of 2. The impedance difference appears at a frequency lower than a few kilohertz, where the interfacial impedance dominates the whole cell impedance. This agrees with our expectation. The phase of measured impedance is not given here, as, in this case, its information is much less straightforward to provide insights into AC electrokinetics.

The next experiment demonstrates the capability of A-P AC EO to collect and immobilize bioparticles onto the electrodes. For the four electrodes shown in Fig. 7, the left two electrodes were energized by unbiased AC signals at 100 Hz, and the right two electrodes were energized by a biased signal:  $0.8V \times (1 + \cos 2\pi \cdot 100 \cdot t)$ , with the right most electrode positively biased. Figure 7

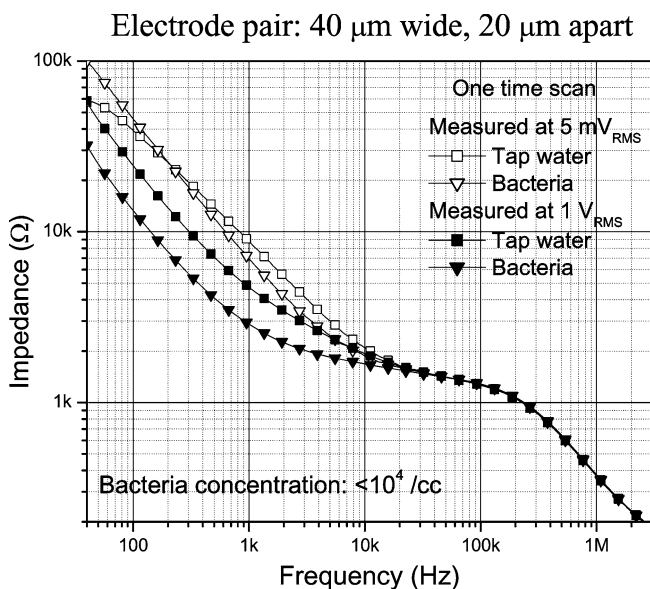


Fig. 6 Impedance measurement of *E. Coli* in tap water

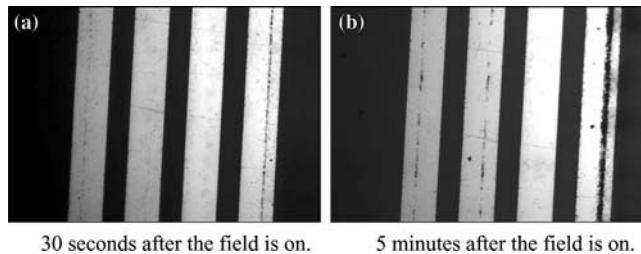


Fig. 7a, b Comparison of particle concentration by electrodes excited by unbiased and biased AC signals: (a) 30 s after the field is on and (b) 5 min after the field is on

shows two frames of particle collection by the two types of applied signals. It can be seen that A-P exhibited much stronger attraction to the particles to the right electrodes than unbiased AC EO, which indicates that A-P AC EO is much more robust in attracting particles to the electrode surface and forming assembly lines. Using an *E. coli* suspension at  $5 \times 10^4$  particles/ml and energizing signals applied as in Fig. 7, the impedances of the two electrode pairs as a function of time are given in Fig. 8. The impedance decreases significantly over time for the right two electrodes while the impedance for the left two electrodes is relatively steady. This is consistent with the observation in Fig. 7 that much more *E. coli* have been collected onto the electrode with time. As the detection signature for bioparticles is a decrease in the impedance, and A-P can continuously collect particles from the bulk of solutions, it is expected that, by measuring the cell impedance with a biased AC signal over a period of several minutes, more bioparticles will be registered by the impedance spectrum, hence, giving rise to the improved sensitivity. This work can be extended to realize a flow-through detection system, as A-P AC EO exhibits the ability to continue attracting particles with particles already assembling on electrode surface.

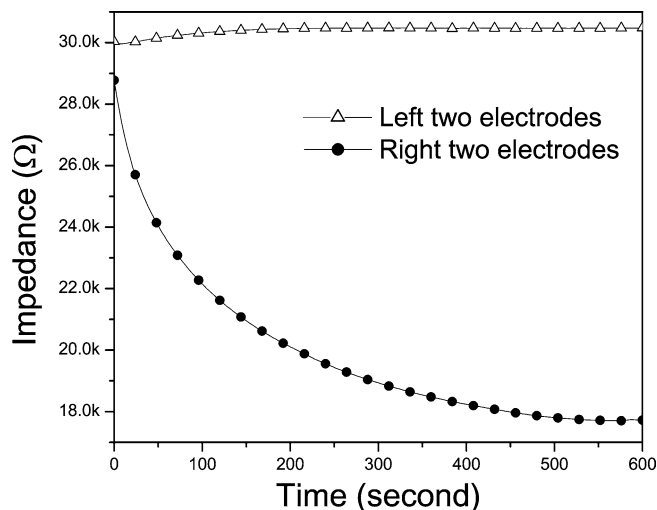


Fig. 8 Impedances of the two pairs of electrodes in Fig. 7 at 100 Hz as a function of time

## 6 Conclusions

This paper describes a novel concept to improve the sensitivity of on-site bioparticle detection by integrating AC electroosmotic (EO) convection with impedance measurements, thus, reducing the diffusion time of bioparticles to the electrodes. Particle and bacterial assembly by AC EO were demonstrated, and directed bioparticle collection by asymmetric electrode polarization were investigated. Incorporating particle assembly with impedance spectroscopy shows promise for enhanced sensitivity in particle detection at point-of-care diagnostic applications.

We are currently developing and optimizing a prototype kit for an EO bioparticle trap based on these preliminary results. The sensitivity and detection time of the kit will be reported in the future.

**Acknowledgements** The bacteria experiments were carried out with the assistance of Dr. David Batigelli, whose assistance is gratefully acknowledged.

## References

- Auerswald J, Knapp HF (2003) Quantitative assessment of dielectrophoresis as a micro fluidic retention and separation technique for beads and human blood erythrocytes. *Microelectron Eng* 67–68:879–886
- Ayliffe HE, Rabbitt RD (2003) An electric impedance based microelectromechanical system flow sensor for ionic solutions. *Meas Sci Technol* 14:1321–1327
- Ayliffe HE, Frazier AB, Rabbitt RD (1999) Electric impedance spectroscopy using microchannels with integrated metal electrodes. *J Microelectromech Syst* 8:50–57
- Buzby JC, Roberts T, Lin CTJ, MacDonald JM (1996) Bacterial foodborne disease: medical costs and productivity losses. *Agricultural Economics Report no. 741*, p 100, Washington, DC, USDA Economic Research Service
- Chang H, Ikram A, Kosari F, Vasmatzis G, Bhunia A, Bashir R (2002) Electrical characterization of micro-organisms using microfabricated devices. *J Vac Sci Technol B* 20:2058–2064
- Chen C-H, Santiago JG (2002) A planar electroosmotic micropump. *J Micro Electro Mech Syst* 11:672–683
- Compton JAF (1987) *Military chemical and biological agents*. Telford Press, Caldwell, New Jersey, p 458
- Gale BK, Frazier AB (1999) Electrical impedance-spectroscopy particle detector for use in microanalysis systems. In: *Proceedings of the SPIE symposium on micromachining and microfabrication: micro fluidic devices and systems*, Santa Clara, California, September 1999, pp 190–201
- Gomez R, Bashir R, Sarikay A, Ladisch MR, Sturgis J, Robinson JP, Geng T, Bhunia AK, Apple HL, Wereley S (2001) Microfluidic biochip for impedance spectroscopy of biological species. *Biomed Microdev* 3:201–209
- Green NG, Ramos A, González A, Morgan H, Castellanos A (2002) Fluid flow induced by nonuniform AC electric fields in electrolytes on microelectrodes. III. Observation of streamlines and numerical simulation. *Phys Rev E* 66:026305
- Hoettges KF, McDonnell MB, Hughes MP (2003) Use of combined dielectrophoretic/electrohydrodynamic forces for biosensor enhancement. *J Phys D Appl Phys* 36:L101–L104
- Hughes MP, Morgan H (1999) Dielectrophoretic characterization and separation of antibody-coated submicrometer latex spheres. *Anal Chem* 71:3441–3445
- Ivnitski D, Abdel-Hamid I, Atanasov P, Wilkins E (1999) Biosensors for detection of pathogenic bacteria. *Biosens Bioelectron* 14:599–624
- Ivnitski D, Abdel-Hamid I, Atanasov P, Wilkins E, Stricker S (2000) Application of electrochemical biosensors for detection of food pathogenic bacteria. *Electroanalysis* 12:317–325
- Keene WE, McAnulty JM, Hoesly FC, Williams LP, Hedberg K, Oxman GL, Barrett TJ, Pfaller MA, Fleming DW (1994) A swimming associated outbreak of hemorrhagic colitis caused by *Escherichia coli* O15:H7 and *Shigella sonnei*. *N Engl J Med* 331:579–584
- Kourkine IV, Ristic-Petrovic M, Davis E, Ruffolo CG, Kapsalis A, Barron AE (2003) Detection of *Escherichia coli* O157:H7 bacteria by a combination of immunofluorescent staining and capillary electrophoresis. *Electrophoresis* 24:655–661
- Mead PS, Slutsker L, Dietz V, McCaig LF, Bresce JS, Shapiro C, Griffin PM, Tauxe RV (2000) Food-related illness and death in the United States. *Center for disease control and prevention, Atlanta, Georgia*
- Minerick AR, Ostafin AE, Chang H-C (2002) Electrokinetic transport of red blood cells in micropillaries. *Electrophoresis* 23:2165–2173
- Morgan H, Hughes MP, Green NG (1999) Separation of submicron bioparticles by dielectrophoresis. *Biophys J* 77:516–525
- Ramos A, Morgan H, Green NG, Castellanos A (1998) AC electrokinetics—a review of forces in microelectrode structures. *J Phys D Appl Phys* 31:2338–2353
- Ramos A, Morgan H, Green NG, Castellanos A (1999) The role of electrodynamic forces in the dielectrophoretic manipulation and separation of particles. *J Electrostat* 47:71–81
- Russell SM (2003) Advances in automated rapid methods for enumerating *E. coli*. *Food Safety magazine*, Feb/Mar 2003. Available at <http://www.foodsafetyjournal.com/issues/0302/colmicro0302.htm>
- Shah J, Wilkins E (2003) Electrochemical biosensors for detection of biological warfare agents. *Electroanalysis* 15:157–167
- Squires TM, Bazant MZ (2004) Induced-charge electro-osmosis. *J Fluid Mech* 509:217–252
- Trau M, Saville DA, Aksay IA (1996) Field-induced layering of colloidal crystals. *Science* 272:706–709
- Wong PK, Chen C-Y, Wang T-H, Ho C-M (2003) An AC electroosmotic processor for biomolecules. In: *Proceedings of the 12th international conference on solid-state sensors and actuators (Transducers 2003)*, June 2003, Boston, Massachusetts, pp 20–23
- Yeh SR, Seul M, Shraiman BI (1997) Assembly of ordered colloidal aggregates by electric-field-induced fluid flow. *Nature* 386:57–59